THE
EMBO
JOURNAL

Ectodomain shedding of the glycoprotein GP of Ebola virus

Olga Dolnik[1,2], Valentina Volchkova[2],
Wolfgang Garten[1], Caroline Carbonnelle[2],
Stephan Becker[1], Jörg Kahnt[3],
Ute Ströher[1], Hans-Dieter Klenk[1] and
Viktor Volchkov[2,*]

[1]Institut für Virologie, Philipps-Universität Marburg, Marburg, Germany, [2]Filovirus Laboratory, University Claude Bernard Lyon-1, INSERM U412, IFR128, Lyon, France and [3]Max-Planck-Institut für terrestrische Mikrobiologie, Marburg, Germany

In this study, release of abundant amounts of the Ebola virus (EBOV) surface glycoprotein GP in a soluble form from virus-infected cells was investigated. We demonstrate that the mechanism responsible for the release of GP is ectodomain shedding mediated by cellular sheddases. Proteolytic cleavage taking place at amino-acid position D_{637} removes the transmembrane anchor and liberates complexes consisting of GP_1 and truncated GP_2 ($GP_{2\Delta}$) subunits from the cell surface. We show that tumor necrosis factor α-converting enzyme (TACE), a member of the ADAM family of zinc-dependent metalloproteases, is involved in EBOV GP shedding. This finding shows for the first time that virus-encoded surface glycoproteins are substrates for ADAMs. Furthermore, we provide evidence that shed GP is present in significant amounts in the blood of virus-infected animals and that it may play an important role in the pathogenesis of infection by efficiently blocking the activity of virus-neutralizing antibodies.

Introduction

Many cellular membrane-anchored glycoproteins are shed from the cell surface upon proteolytic cleavage, a process referred to as ectodomain shedding (Hooper et al, 1997; Müllberg et al, 2000). This process affects structurally and functionally different proteins, including growth factors, precursors of cytokines and their receptors, as well as ectoenzymes and cell adhesion molecules (Hooper et al, 1997; Schloendorf and Blobel, 1999). For instance, membrane-anchored receptors for growth factors and cytokines are shed from the cell surface as soluble molecules and still retain the ability to bind their ligands. Furthermore, cytokines, which are synthesized as transmembrane proteins, have to be cleaved and shed to achieve systemic availability (Rose-John and Heinrich, 1994). The appropriate balance between the membrane-bound and the soluble form of a protein may therefore be of high significance for its physiological role (Blobel, 2002). However, ectodomain shedding may also have undesirable consequences by promoting diseases. For example, increased concentrations of shed tumor necrosis factor α (TNF-α), which is a critical inflammatory mediator, have been shown in patients with active Crohn's disease and rheumatoid arthritis (Elliott et al, 1994; Van Dullemen et al, 1995).

Ectodomain shedding is mediated by members of the metzincin superfamily of zinc-dependant metalloproteases that include the matrix metalloproteases (MMPs) and ADAMs (for a disintegrin and metalloprotease) (Blobel, 2000). MMPs are mainly involved in regulated reconstruction of the extracellular matrix during development, differentiation, and wound healing, whereas ADAMs play an important role in development, fertilization, myoblast fusion, and cell–cell interactions in addition to ectodomain shedding. To date, the best-characterized ADAM is the TNF-α-converting enzyme (TACE or ADAM 17). TACE is expressed in many different tissues like heart, placenta, testes, and ovaries, and also in monocytes, T cells, neutrophils, and endothelial cells, and is involved in many physiological processes (Black et al, 1997). Analysis of $TACE^{\Delta Zn/\Delta Zn}$ mice lacking functional TACE showed defects not only in TNF-α release but also in shedding of TGF-α, L-selectin, and TNF-receptor p75 (Peschon et al, 1998). In addition, TACE has been implicated in the ectodomain shedding of IL-1 receptor, Notch receptor, and also in the cleavage of amyloid precursor protein (Buxbaum et al, 1998; Brou et al, 2000; Reddy et al, 2000). Involvement of cellular sheddases in the ectodomain shedding of viral surface glycoproteins was hitherto not reported, although the release of soluble glycoproteins has been described for several viruses.

EBOV is a member of the Filoviridae, a family of enveloped, nonsegmented, negative-stranded RNA viruses. The EBOV genome encodes seven structural proteins and one nonstructural protein, sGP. The pathogenesis of hemorrhagic fever caused by EBOV (mortality rates up to 90%) is only partially understood. It has been suggested, however, that the inability of the host immune system to clear infection is a major factor responsible for the dramatic course of the disease (Peters, 1996).

The GP gene of EBOV encodes two glycoproteins. The small nonstructural glycoprotein sGP is the primary product of the GP gene, which is secreted from infected cells as a disulfide linked homodimer (Volchkov et al, 1995; Sanchez et al 1996, Volchkova et al, 1998). Surface GP of EBOV is expressed from the same GP gene by a mechanism of cotranscriptional RNA editing (Volchkov et al, 1995). sGP is structurally and functionally distinct from surface GP and is

*Corresponding author. Filovirus Laboratory, University Claude Bernard Lyon-1, INSERM U412, 21 avenue Tony Garnier, 69365 Lyon, France.
Tel.: +33 437 28 2450; Fax: +33 437 28 2459;
E-mail: volchkov@cervi-lyon.inserm.fr

not recognized by virus-neutralizing monoclonal anti-GP antibodies (Maruyama *et al*, 1999). GP is a type I transmembrane protein that is assembled as a homotrimer and constitutes the spikes on virions (Sanchez *et al*, 1998; Volchkov *et al*, 1998b). Synthesis of GP involves proteolytic processing by the proprotein convertase furin at a polybasic cleavage site. Mature GP consists of two fragments, GP_1 (501 aa) and GP_2 (175 aa), that are linked by a disulfide bond (Volchkov *et al*, 1998b; Jeffers *et al*, 2002). GP mediates virus entry by receptor binding and membrane fusion (Yang *et al*, 1998; Ito *et al*, 1999; Chan *et al*, 2001; Alvarez *et al*, 2002). Evidence that recombinant GP induces cell detachment suggests that GP is a determinant of pathogenicity (Chan *et al*, 2000; Yang *et al*, 2000).

In this study, we demonstrate that proteolytic cleavage of surface GP of EBOV results in shedding of significant amounts of $GP_{1,2\Delta}$, the soluble form of GP. We also show that the cellular zinc-dependent metalloprotease TACE, a member of the ADAM proteinase family, is involved in the cleavage of GP and provide evidence that shed GP released during infection efficiently blocks virus-neutralizing antibodies.

Results

Soluble GP of EBOV contains a truncated GP_2 subunit

Release of GP from EBOV-infected cells was first described by Volchkov *et al* (1998a). To understand the molecular mechanism of release, RK-13 cells were infected with recombinant vaccinia virus vSCGP8 expressing GP, labeled 10 h p.i., and chased for 6 h. Cells and culture medium were collected separately, and soluble proteins from the medium were separated by ultracentrifugation. GP from cells and medium was immunoprecipitated using rabbit anti-GP_2 antibodies and analyzed under reducing conditions by SDS–PAGE. In addition to GP_2, a protein with slightly higher electrophoretic mobility was identified in the medium, which was designated $GP_{2\Delta}$ (Figure 1A). Sedimentation analysis of the medium showed that $GP_{2\Delta}$ remained in the supernatant fraction, whereas GP_2 was found only in the pellet fraction. GP in the pellet represents membrane-associated $GP_{1,2}$ complexes released into the medium as virosome-like particles (Volchkov *et al*, 1998a). Sucrose gradient flotation analysis confirmed that $GP_{2\Delta}$ is present in a soluble form (see Supplementary Figure 1). Irrespective of the anti-GP antibodies used for immunoprecipitation (anti-GP_2 or monoclonal anti-GP antibody KZ52), soluble fractions always showed comparable amounts of GP_1 and $GP_{2\Delta}$, indicating that the subunits are linked in the $GP_{1,2\Delta}$ complexes as they are in membrane-bound $GP_{1,2}$. In order to demonstrate that release of soluble $GP_{1,2\Delta}$ is also observed in EBOV infection and not specific for the recombinant expression system, Vero E6, HeLa, or RK-13 cells were infected with EBOV, and culture medium was harvested 5 days p.i. The presence of virus-associated GP_2 and $GP_{2\Delta}$ in the medium was shown by immunoblot analysis using anti-GP_2 antibody. $GP_{2\Delta}$ was detected with all three cell lines depending on the susceptibility of cells for EBOV replication (Figure 1B). The amount of soluble $GP_{1,2\Delta}$ in the supernatants of all tested cell lines represents up to 20% of the total GP released from virus-infected cells.
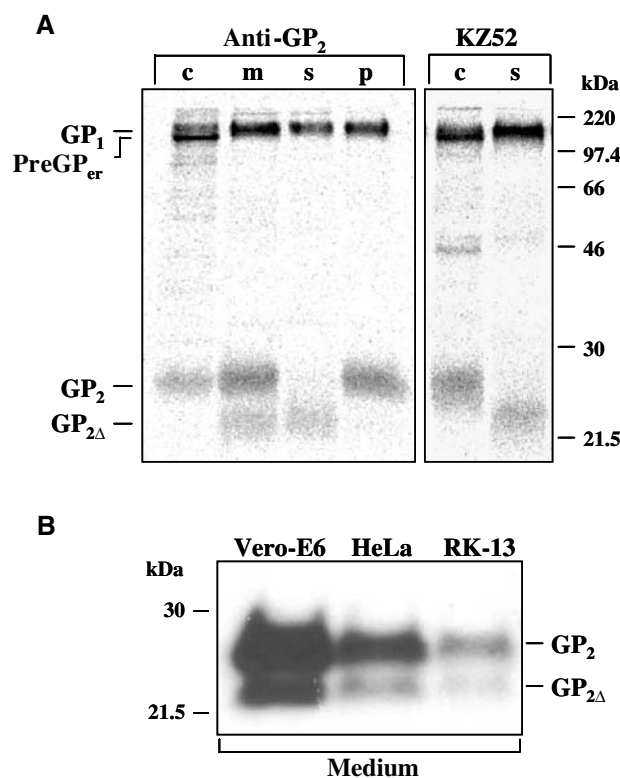

Figure 1 Release of soluble EBOV $GP_{1,2\Delta}$ complexes. (**A**) RK-13 cells were infected with vSCGP8, pulse labeled 10 h p.i. and chased for 6 h. Culture medium (m) and cells (c) were collected separately. Soluble (s) and membrane-bound (p) proteins were separated by ultracentrifugation (25 000 rpm, 1 h, 4°C). Labeled proteins were immunoprecipitated using rabbit anti-GP_2 Igs or human monoclonal antibody KZ52. (**B**) Western blot analysis of culture medium from EBOV-infected Vero E6, HeLa, and RK-13 cells.

GP_2 and $GP_{2\Delta}$ have the same glycosylation pattern

It was then of interest to investigate whether a difference in glycosylation pattern was responsible for the appearance of GP_2 with low molecular mass ($GP_{2\Delta}$). The GP_2 subunit has two potential N-linked glycosylation sites at positions 563 and 618. Treatment of GP_2 with Endo H and PNGase F showed that both sites are glycosylated, one containing a complex type, the other a high-mannose type oligosaccharide (Figure 2A). To identify the attachment site of each type, two recombinant vaccinia viruses expressing mutated GP were generated, and GP_2 from infected cells was analyzed using endoglycosidase treatment. Each mutant had only one glycosylation site, GP618N/T at position 563 or GP563N/T at position 618. The GP618N/T mutant showed sensitivity to Endo H and PNGase F digestion, indicating that the high-mannose type oligosaccharide is bound at position 563. In contrast, GP_2 from the GP563N/T mutant showed Endo H resistance and was sensitive only to PNGase F treatment, indicating that the complex type oligosaccharide is bound at position 618 (Figure 2A).

To confirm that soluble GP released from EBOV-infected cells has the same glycosylation pattern, Vero E6 cells were infected with EBOV, culture medium was collected 5 days p.i., and membrane-bound and soluble GP were separated by ultracentrifugation. Culture medium, and supernatant and pellet obtained after centrifugation were analyzed by immunoblotting using anti-GP_2 antibody followed by treatment
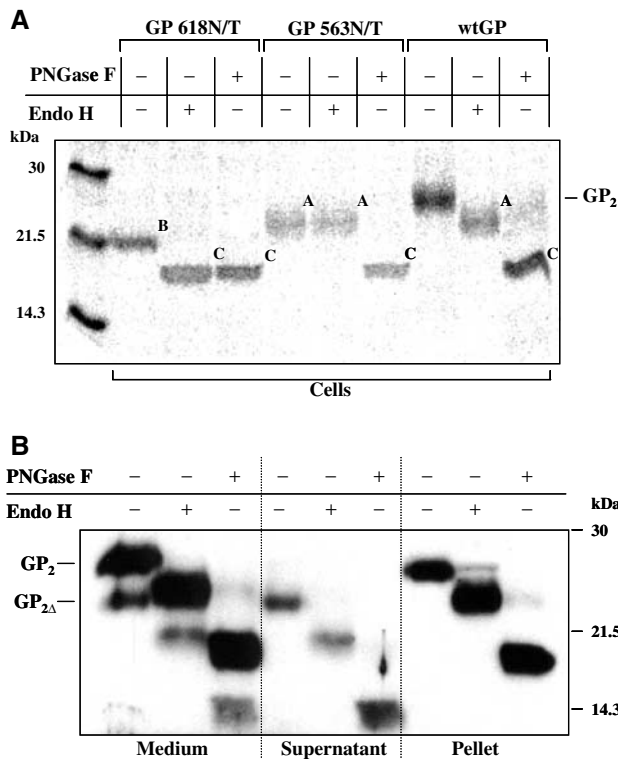
Figure 2 Analysis of glycosylation pattern of GP$_2$ and GP$_{2\Delta}$. (**A**) RK-13 cells were infected with vSCGP8 (wtGP) or vaccinia viruses expressing glycosylation mutants (GP618N/T and GP563N/T) and subjected to pulse-chase labeling and immunoprecipitation with horse anti-EBOV Igs followed by endoglycosidase treatment with Endo H or PNGase F. Forms of GP$_2$ differing in N-glycosylation pattern are indicated as follows: A—containing only complex type oligosaccharides, B—containing only high-mannose type oligo-saccharides, C—completely deglycosylated molecules. (**B**) Culture medium from Vero E6 cells infected with EBOV was ultracentri-fuged, and pellet and supernatant were collected separately. Samples were either treated with Endo H or PNGase F or used untreated. Proteins were analyzed by Western blot.

with Endo H or PNGase F (Figure 2B). Both, GP$_{2\Delta}$ and GP$_2$ showed the same glycosylation patterns, confirming that the difference in molecular mass identified by SDS–PAGE is not dependent on glycosylation.

GP$_{1,2\Delta}$ is released from the cell surface

In order to investigate the kinetics of the release of GP$_{1,2\Delta}$ and also to clarify whether this form of GP is generated intracel-lularly or at the cell surface, pulse-chase labeling experiments were performed. RK-13 cells were infected with vSCGP8, metabolically labeled 7 h p.i., and chased for different time intervals. GP from the medium and cell was analyzed by immunoprecipitation using anti-GP antibodies. During con-version of the endoplasmic reticulum precursor preGP$_{er}$ into the Golgi precursor preGP and subsequently into mature GP$_{1,2}$ complexes, no GP$_{2\Delta}$ was detected intracellularly. GP$_{1,2\Delta}$ complexes were first identified in the culture medium at about 90 min after pulse (Figure 3A). Release of GP$_{1,2}$ complexes in virosomes was observed later. The absence of GP$_{2\Delta}$ within cells supported the notion that GP$_{1,2\Delta}$ is released into the medium from the cell surface. For further analysis of the GP release, surface labeling experiments were performed. RK-13 cells were infected with vSCGP8 and surface biotiny-
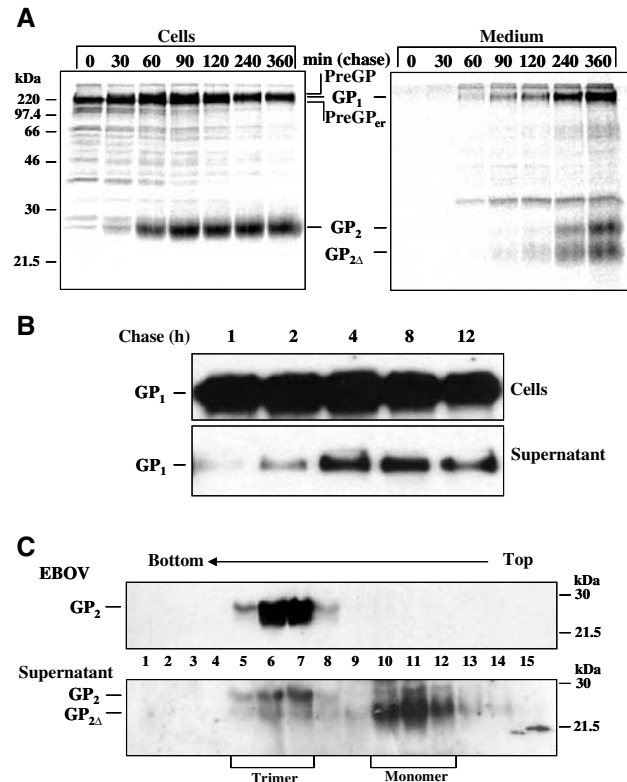

Figure 3 Kinetics of release and oligomeric structure of soluble GP. (**A**) RK-13 cells infected with vSCGP8 were pulse-chase labeled and proteins were immunoprecipitated from cells (left panel) and medium (right panel). (**B**) Surface biotinylation of RK-13 cells expressing EBOV GP. Release of biotin-labeled GP from the cell surface into culture supernatant was observed at indicated time intervals. (**C**) Analysis of the oligomeric structure of shed GP. Vero E6 cells were infected with EBOV. At 5 days p.i., virus from culture medium was pelleted through a 20% sucrose cushion, and subse-quently the supernatant and virus were analyzed by ultracentrifu-gation at linear sucrose gradients in the presence of 1% NP-40 and 0.4% DOC. Fractions 1–15 were collected from the bottom and analyzed by Western blot. Due to the effect of several detergents present in the samples such as NP-40, DOC, and finally SDS, the bands appeared slightly more diffused compared to other analyses.

lated 10 h p.i. Culture supernatants and cells were collected separately at different time intervals. GP was immunopreci-pitated and analyzed by SDS–PAGE followed by detection of biotinylated GP with HRP-coupled streptavidin. Kinetic stu-dies showed that soluble GP was released from the cell surface and that most of the GP remained membrane-asso-ciated even 12 h after labeling (Figure 3B). A maximum of soluble GP was detected 4 h post labeling. Prolonged incuba-tion did not lead to increased release. Taken together, these data suggest that GP$_{1,2\Delta}$ complexes are released from the cell surface due to proteolytic cleavage by cellular proteases.

Previously, it has been shown that the spikes of filoviruses are GP trimers (Sanchez *et al*, 1998). In order to determine whether GP$_{1,2\Delta}$ is present in solution as an oligomer, centri-fugation analysis using linear sucrose gradients was per-formed. Culture medium from EBOV-infected cells was clarified from virus particles by centrifugation through a 20% sucrose cushion. Supernatant and virus pellet were solubilized with 1% NP-40 and 0.4% DOC and subjected to ultracentrifugation on linear 5–25% sucrose gradients. Western blot analysis of the fractions collected from the

bottom of the gradient using anti-GP$_2$ antibody showed that GP from virions is present only in fractions 5–8 (Figure 3C) corresponding well to previous work where GP was identified as a trimer (Sanchez *et al*, 1998). Soluble GP from culture medium was found at the same position in the gradients and therefore is also in a trimeric form. However, after solubilization and ultracentrifugation in the presence of 1% NP-40 and 0.4% DOC, most of GP$_{1,2\Delta}$ was detected in lighter sucrose fractions, obviously representing dimers and monomers. These results indicate that GP$_{1,2\Delta}$ trimers appear to be rather labile and easily dissociated compared to virion GP$_{1,2}$.

EBOV GP is cleaved at amino-acid position D$_{637}$

To map the region of the putative cleavage site, plasmids encoding GP deletion mutants were generated, and expression of GP was analyzed. ΔTM is a mutant lacking the transmembrane anchor. Δ640 and Δ630 are mutants lacking, in addition, 10 or 20 adjacent amino acids (Figure 4A). After expression in HeLa cells, GP from medium was subjected to PNGase F treatment and Western blot analysis (Figure 4B). Soluble GP released from EBOV-infected HeLa cells (GP$_2$) and GP from viral particles were used as wild-type controls. As indicated in Figure 4B, GP$_{2\Delta}$ released from EBOV-infected HeLa cells migrated on polyacrylamide gels at a position between Δ630 GP$_2$ and ΔTM GP$_2$. These data allowed mapping of the cleavage position to a region of 10 aa between F$_{630}$ and D$_{640}$ (Figure 4A and B).

To determine the exact position of the cleavage site, Vero E6 cells were infected with EBOV, culture medium was collected 5 days p.i., and soluble GP$_{1,2\Delta}$ was purified from the medium by affinity chromatography using anti-GP$_2$ antibody. Additional purification was achieved using wheat germ lectin agarose chromatography. Finally, N-glycans were removed from purified GP$_{1,2\Delta}$ complexes by PNGase F treatment. GP$_1$ and GP$_{2\Delta}$ subunits were separated after incubation with DTT, and sulfide groups of cysteine residues were blocked by alkylation with iodacetamide. Absence of the linkage between subunits in treated samples was confirmed by SDS–PAGE analysis performed under nonreducing conditions followed by silver staining and by immunoblotting using anti-GP$_2$ antibody that showed a single GP$_2$-specific band migrating as a protein of about 14.3 kDa (Figure 4C). Analysis of this sample by MALDI-TOF MS revealed four peaks in the mass spectra (Figure 4D). The broad signal around 18 000 is typical for protein degradation products resulting from laser desorption. Two peaks corresponded to the PNGase F added to the sample. One of these peaks represents a single protonated ion $[M+H]^+$ with a mass/charge ratio of 35 157. It corresponds well with the theoretical mass of PNGase F (34 836 or 35 094 following alkylation of cysteine residues). The experimental error was therefore 0.18%. A second PNGase F peak represents a doubly protonated ion $[M+2H]^{2+}$ with a mass/charge ratio only half as big (17 606). Truncated GP$_{2\Delta}$ showed an average mass of 15 551 from which the mass of the attached carboxyamidoyl groups had to be subtracted. The resulting mass of 15 336 is in good agreement with the theoretical mass of 15 332 for GP$_{2\Delta}$ terminating at D$_{637}$ (Figure 4D).

In order to confirm the data obtained by mass spectrometry and to define a recognition motif required for the cleavage of EBOV GP, several recombinant vaccinia viruses expressing GP mutants with single amino-acid changes in the

immediate vicinity of D$_{637}$ were generated. RK-13 cells were infected with these recombinant vaccinia viruses, cells were metabolically labeled 7 h p.i., and chased for the next 10 h. GP from cells and medium was immunoprecipitated with specific antibodies, proteins were separated by SDS–PAGE, and GP$_2$ was quantified on a Bio-imager using PC-Bas software. GP expression levels were comparable for most mutants, but there were differences in the extent of GP shedding into the medium (Figure 4E). In case of mutants 634T/I, 635L/V, 636P/A, 639G/V, and del634–640, amounts of shed GP were reduced up to 60% indicating that the amino-acid residues T$_{634}$, L$_{635}$, P$_{636}$, and G$_{639}$ may contribute to recognition and cleavage. Interestingly, two other mutants, 637D/V and 637D/L, showed a substantial increase in GP shedding (see Supplementary Figure 3). Exchange of the negatively charged aspartate to an uncharged residue at positions D$_{632}$, D$_{640}$, or D$_{642}$ did not result in increase of shedding, however.

Inhibitors of zinc-dependent metalloproteinases prevent GP shedding

To characterize the cellular enzyme responsible for the shedding of GP$_{1,2\Delta}$, a number of known inhibitors of proteinases were tested (Table I). RK-13 or 293 cells expressing GP were pulse labeled and chased with medium containing protease inhibitors. The medium was collected 8 h after addition of inhibitors, and GP was precipitated using specific antibodies. Proteins were separated by SDS–PAGE, and GP$_{2\Delta}$ bands were quantified by Bio-imaging. Several compounds showed more than 50% inhibition of GP shedding. The highest inhibitory effects were observed with the hydroxamic acid-based inhibitors: BB2516 used at a concentration of 0.5 μM, and GM 6001 and MMP-8 inhibitor I used at a concentration of 5 μM. Other inhibitors, such as MMP-3 inhibitor II, CGS-27023A, and TAPI-I, reduced GP shedding at higher concentrations (25–50 μM). The effect of all these inhibitors was concentration dependent (see Supplementary Figure 2). The inhibition of shedding by 1,10-phenanthroline (1 mM) was reversible after addition of zinc ions. Natural inhibitors of matrix metalloproteinases such as TIMP-1, -2, -3, and -4 did not inhibit GP shedding. Taken together, these data suggest that the protease responsible for EBOV GP shedding belongs to the proteinase superfamily of zinc-dependent metalloproteinases.

TACE is involved in GP shedding

TACE is a widely expressed protease that has been shown to cleave the ectodomains of different cellular transmembrane glycoproteins (Black *et al*, 1997). This enzyme is also expressed by cells of the mononuclear phagocyte system that are the primary target for EBOV infection. Involvement of TACE in EBOV GP shedding was first investigated on 293 cells. Although there is some GP shedding in 293 cells resulting, most likely, from endogenous TACE, there was a distinct enhancement of shedding when the enzyme was overexpressed. For this purpose, cells were transfected simultaneously with two plasmids, one expressing EBOV GP and another expressing recombinant TACE. Whereas synthesis of GP was not affected by coexpression of TACE, we observed an increase of 70% in shedding of GP$_{1,2\Delta}$ (Figure 5A). To further confirm involvement of TACE in GP shedding, we also performed conditional TACE knockout using ASOs. 293 cells were infected with vSCGP8 and subsequently
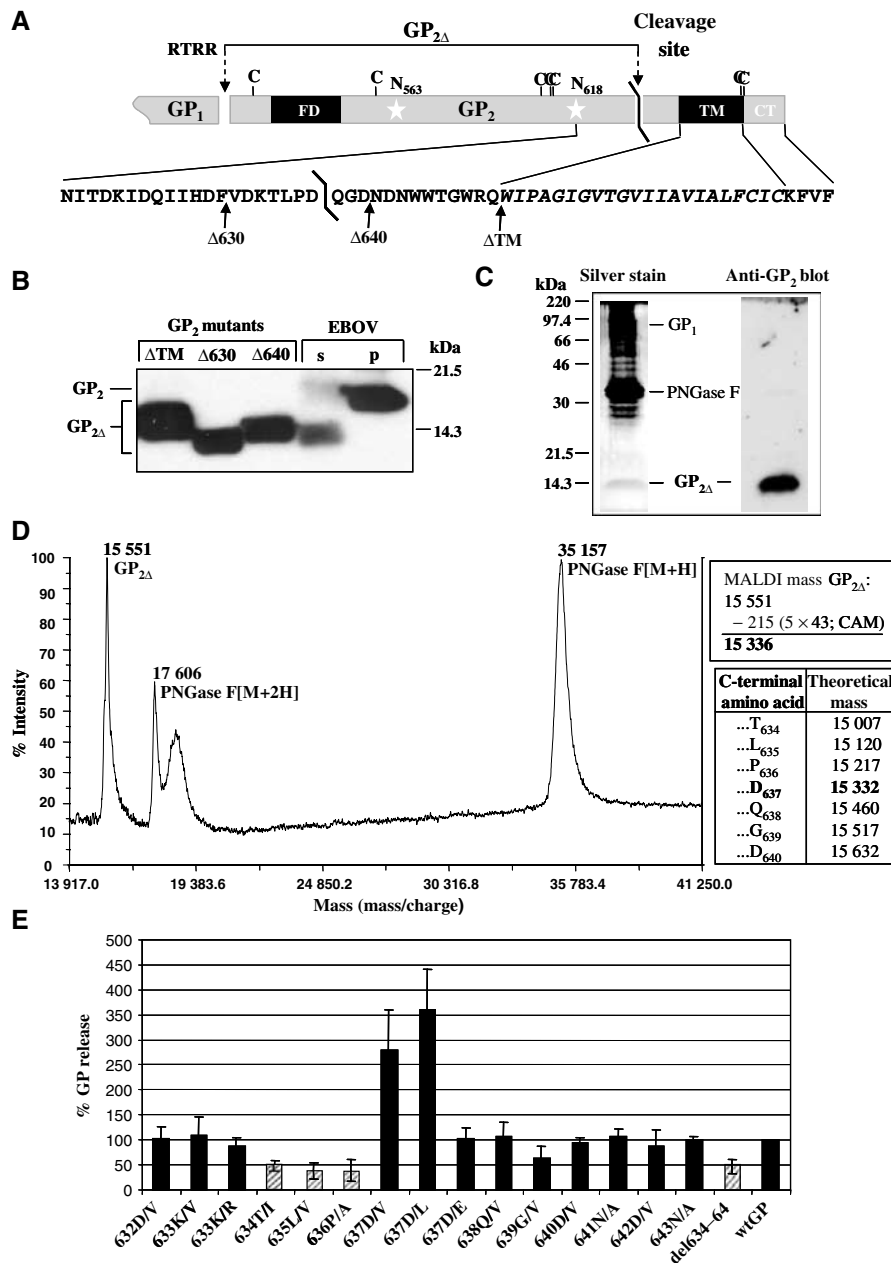
Figure 4 Determination of the carboxy-terminus of $GP_{2\Delta}$. (**A**) Schematic illustration of EBOV GP_2. Subtilisin-like cleavage site (RTRR), shedding cleavage site ($D_{637}-Q_{638}$), position of carboxy-terminal deletion mutants (ΔTM, Δ630, Δ640), cysteine residues (C), N-glycosylation sites N_{563} and N_{618} (white stars), transmembrane anchor (TM), cytoplasmic tail (CT), and fusion peptide (FD) are indicated. (**B**) Western blot analysis of GP deletion mutants. Culture medium from HeLa cells infected with vTF7-3 and transfected with pGEMmGP8/ΔTM, pGEMmGP8/Δ630, or pGEMmGP8/Δ640 was treated with PNGase F and subjected to Western blot analysis. GP_2 from virus particles (p) and shed $GP_{2\Delta}$ from EBOV-infected HeLa cells (s) were used as controls. (**C**) SDS–PAGE analysis of purified soluble GP under nonreducing conditions. The left panel shows silver staining and the right panel immunodetection with anti-GP_2 Igs. (**D**) Analysis of purified GP preparation by MALDI-TOF MS. $GP_{2\Delta}$ and PNGase F peaks are indicated. Upper box: $GP_{2\Delta}$ mass after subtraction of carboxyamidoyl group mass (CAM); lower box: theoretical masses of $GP_{2\Delta}$ with indicated carboxy-terminal amino acid. (**E**) Influence of amino-acid exchanges on GP shedding. RK-13 cells infected with vSCGP8 (wtGP) or virus mutants with indicated exchanges were labeled and analyzed by immunoprecipitation. Quantification of released $GP_{2\Delta}$ was performed using Bio-imaging. Representative results from individual experiments are presented as mean values ($\pm$s.d.).

transfected with different anti-TACE ASO. Culture medium and cells were collected separately after pulse-chase labeling and subjected to immunoprecipitation with anti-GP antibodies. Anti-TACE ASO treatment reduced GP shedding by 30% (ASO4) to 45% (ASO2) as compared to untreated controls (Figure 5B). Treatment with ASO2M and ASO4M, which had four nucleotide mismatches with human *TACE*, did not affect GP shedding.

Final proof for the involvement of TACE in shedding of GP was obtained in experiments with the mouse fibroblast cell line EC-2 expressing nonfunctional TACE due to a deletion in the zinc-binding domain (Peschon *et al*, 1998). The level of GP expression in these TACE-deficient fibroblasts was comparable to other cell lines, but GP shedding was almost abrogated. However, shedding was restored after coexpression of GP and TACE cDNA (Figure 5C). This experiment

Table I Influence of protease inhibitors on GP shedding

Inhibitor	Inhibitory effect on $GP_{1,2\Delta}$ shedding
TAPI-I (50 μM)	+
1,10-Phenanthroline (1 mM)[a]	+
EDTA (5 mM)	−
EGTA (5 mM)	−
Phosporamidon	−[b]
α-1-Antichymotrypsin (4 μM)	−
Captopril (10 μM)	−
BB2516 (500 nM)	+
GM 6001 (5 μM)	+
TIMP-1, -2, and -4 (200 nM)	−
TIMP-3	−[b]
MMP-2 inhibitor I (100 μM)	−
MMP-3 inhibitor II (50 μM)	+
MMP-8 inhibitor I (5 μM)	+
CGS-27023A (25 μM)	+

+Inhibition of $\geqslant 50\%$ at the indicated inhibitor concentration.
−No inhibition at the indicated inhibitor concentration.
[a]Inhibition by 1,10-phenanthroline is reversible by equimolar Zn^{2+} addition.
[b]Inhibitory effect less than 50% and no dependence on inhibitor concentration.

clearly demonstrates that TACE is a cellular secretase involved in the shedding of EBOV GP.

Soluble GP is present in the blood of infected guinea pigs and inhibits the neutralizing activity of the EBOV-specific antibody KZ52

Immunoprecipitation of shed GP by the virus-neutralizing antibody KZ52 (Figure 1A) provided the first evidence that it may serve as a decoy during EBOV infection. To investigate whether shed GP can prevent neutralization of EBOV, a neutralization inhibition assay was established. In this assay, KZ52 antibody neutralized EBOV infectivity (>60%) at a concentration of 0.6 μg/ml as previously described by Maruyama *et al* (1999). The virus-neutralizing activity of KZ52 was completely blocked in the presence of equimolar amounts of affinity-purified shed GP (Figure 6A). The inhibitory effect depended specifically on the interaction of GP with the antibody as indicated by the observation that it was abrogated when the amount of GP was reduced to a molar GP/antibody ratio of 1/10. As shown in the control experiments, shed GP did not markedly affect virus replication, when added alone to infected cell cultures.

To demonstrate that shed GP is also present in the blood of infected animals, guinea pigs were infected with a guinea pig-adapted EBOV variant, and blood samples were collected 6 and 9 days p.i. Release of the virus into the blood was confirmed by virus titrations ($\sim 2 \times 10^2$ and $\sim 5 \times 10^4$ infectious units, respectively) and by Western blot analysis using anti-VP40 antibodies. The low VP40 signal and the inability to detect virion GP_2 correspond to the relatively low virus titers found in the blood. In contrast, there was a remarkably high amount of truncated $GP_{2\Delta}$ (Figure 6B). Comparative analysis of deglycosylated glycoproteins obtained from cell culture medium and blood clearly demonstrated that the latter one was $GP_{2\Delta}$. It has to be pointed out that the increase in the amount of shed GP detected between days 6 and 9 correlates well with the course of illness and the lethal
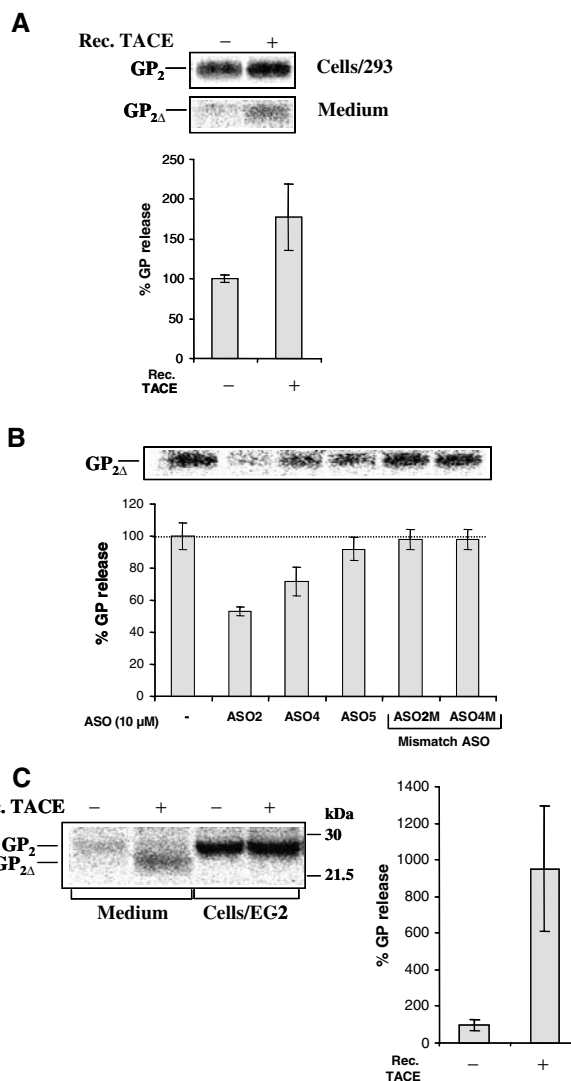

Figure 5 Involvement of TACE in EBOV GP shedding. (**A**) 293 cells were transfected with pcDNA3.1-GP or co-transfected with pcDNA3.1-GP and pcDNA3Mu TACE FL. At 36 h p.t., cells were pulse labeled and chased for 8 h. Labeled proteins were analyzed by immunoprecipitation. (**B**) 293 cells were infected with vSCGP8 and subsequently transfected with ASOs. Mismatch ASO2M and ASO4M were used as negative controls. At 7 h p.t., cells were labeled and chased for 8 h. Proteins from culture medium were analyzed by immunoprecipitation. (**C**) EC-2 cells (TACE$^{\Delta Zn/\Delta Zn}$) lacking functional TACE were transfected with pcDNA3.1-GP or co-transfected with pcDNA3Mu TACE FL and pcDNA3.1-GP. Cells were pulse-chase labeled 18 h p.t., and medium and cells were analyzed by immunoprecipitation. For all three panels (A–C) statistical analysis using at least three independent experiments has been performed. Mean values of GP release (% ±s.d.) are shown in bars. Quantification of the released $GP_{2\Delta}$ was performed using Fuji BAS 1000 Bio-Imaging Analyzer.

outcome at day 9 p.i. This suggests that shed GP plays an important role in pathogenesis.

Discussion

Soluble glycoproteins have been described for a number of viruses (Morimoto *et al*, 1993; Malvoisin and Wild, 1994; Roberts *et al*, 1994), but little is known about the mechanisms and the biological significance of their release.
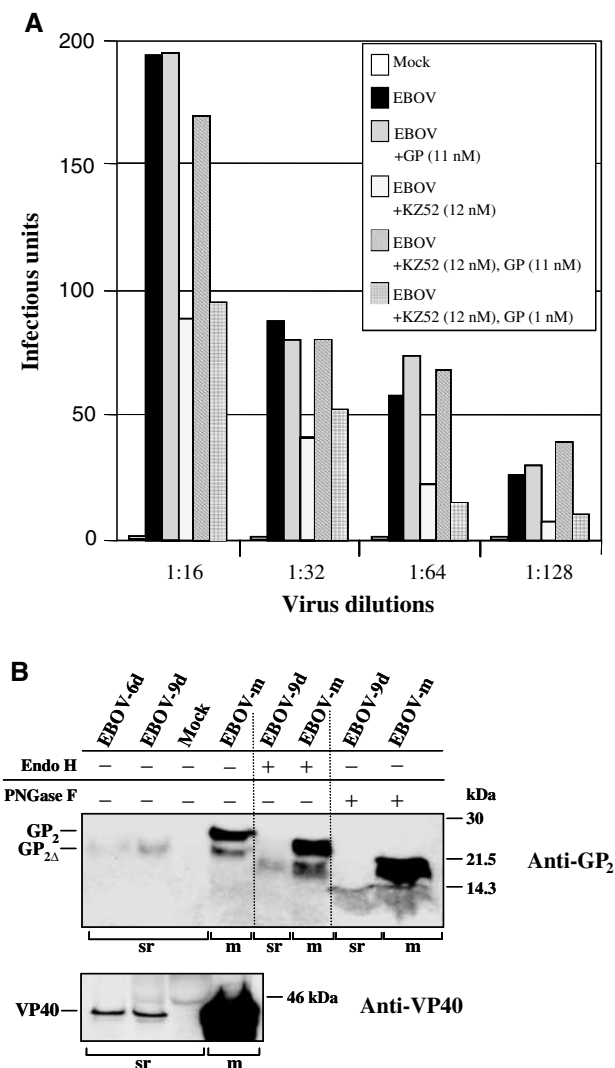
A

B

Figure 6 $GP_{1,2\Delta}$ is present in the blood of infected guinea pigs and is able to inhibit the virus-neutralizing activity of human monoclonal antibody KZ52. (**A**) Virus neutralization inhibition assays were performed using different EBOV dilutions in the presence of KZ52 antibody or shed GP or both at indicated concentrations. Total number of infectious units obtained for each reaction is indicated in bars. (**B**) Vero E6 cells were infected with EBOV and culture medium collected 5 days p.i. (EBOV-m). Guinea pigs (strain Hartley) were infected intraperitoneally with 1×10^3 PFU/animal of guinea pig-adapted EBOV (Volchkov *et al*, 2000). At days 6 and 9 p.i. (EBOV-6d, EBOV-9d), GP_2, $GP_{2\Delta}$, and VP40 were identified in sera (sr) and in culture medium (m) by Western blot analysis using specific antibodies. Samples from blood (at day 9 p.i.) and culture medium were either treated with Endo H or PNGase F or used untreated.

Premature termination of translation has been suggested to be responsible for release of the carboxy-terminally truncated G protein of VSV (type I transmembrane glycoprotein) (Grünberg *et al*, 1991). Solubilization of the G protein of respiratory syncytial virus (RSV), a type II transmembrane glycoprotein, was thought to depend on the use of an alternative translation start codon that made the protein sensitive to cleavage by signal peptidase (Roberts *et al*, 1994).

Here we show that EBOV glycoprotein GP is effectively shed from infected cells owing to proteolytic cleavage within the transmembrane subunit GP_2 that removes the transmembrane anchor and liberates the ectodomain consisting of GP_1

and truncated $GP_{2\Delta}$. GP containing truncated GP_2 was detected exclusively extracellularly indicating that cleavage takes place at the cell surface. The kinetics of shedding suggested that cleavage occurs immediately after the arrival of GP at the plasma membrane. Interestingly, the fraction of released GP did not increase upon further exposure at the cell surface, suggesting conversion from a cleavage-sensitive to a cleavage-insensitive form. It has been recently shown that mature GP is incorporated at the plasma membrane into lipid rafts (Bavari *et al*, 2002), but it remains to be seen if protection from shedding depends on raft association. To determine the exact cleavage site, shed GP was purified from culture supernatants of virus-infected cells using affinity column chromatography. Mass spectrometrical analysis of purified GP showed that the carboxy-terminus of truncated GP_2 is Asp at position 637 ($LPD_{637}\downarrow Q_{638}GD$). Single amino-acid substitutions placed around the cleavage site modulated the intensity of GP shedding. None of the introduced mutations, however, led to complete blockage of GP cleavage and shedding. Interestingly, exchange of the negatively charged Asp at position 637 to uncharged residues resulted in an increase of GP shedding. The generated sequence LPVQ corresponds to the known cleavage site of the IL-6 receptor recognized by TACE, a member of the ADAM family of zinc-dependent metalloproteinases (Althoff *et al*, 2000). The notion that such an enzyme is involved in GP shedding was further supported by proteinase inhibition studies. Direct evidence for the involvement of TACE was obtained by the finding that GP shedding was drastically reduced in the TACE-deficient cell line EC-2 (Peschon *et al*, 1998), but could be restored by transfection with plasmids encoding TACE. Additional proof for TACE as a post-translational processing enzyme for EBOV GP was achieved by conditional knockout experiments using TACE-specific ASOs. Although these observations, taken together, clearly show that TACE is responsible for GP release, we cannot completely rule out that other shedding enzymes, such as ADAM 9 and ADAM 10, also play a role. However, it is unlikely that matrix metalloproteinases (MMPs) that also belong to the metzincin superfamily are involved in shedding of GP because none of the tested natural inhibitors of these enzymes inhibited the release of GP.

Proteases releasing proteins from the cell surface like TACE are designated sheddases or secretases (Hooper *et al*, 1997). In contrast to many other cellular proteases (subtilisin-like endoproteases for instance), there is no apparent sequence homology between the cleavage sites recognized by secretases (Hooper *et al*, 1997; Müllberg *et al*, 2000). The cleavage sites of TACE, for example, on TNF-α, L-selectin, and APP do not show a consensus sequence (Black *et al*, 1997; Buxbaum *et al*, 1998; Peschon *et al*, 1998). The distance between the cleavage site and the transmembrane anchor appears to be more important for the efficiency of shedding than a strict sequence motif, although the distance may vary considerably with different proteins, ranging from eight residues (TNF-R-p55; IL-6R and TGF-α) to 36 residues (rat β4 heregulin) (Ehlers *et al*, 1996). Folded domains have never been shown to be affected by shedding enzymes, presumably because the proteases have no access to potential cleavable sequences (Althoff *et al*, 2001). Moreover, structural changes within the juxtamembrane domain, which increase molecular dynamics and disorder, appear to render a protein susceptible to cellular sheddases. The cleavage site of EBOV GP

fulfills these requirements, since it is located 13 aa upstream of the transmembrane anchor (W_{651}-C_{672}) and five residues downstream of an α-helical domain (W_{615}-F_{630}).

As has been pointed out above, release of cellular proteins into the extracellular environment is a control mechanism of numerous cell functions. Likewise, GP shedding may play an important regulatory role in virus replication and pathogenesis. Enhanced cleavage, as observed here with two mutants of GP, should reduce the amount of GP on the cell surface available for formation of virus particles. Less-efficient cleavage or even the absence of cleavage may also have serious consequences, since EBOV GP is cytotoxic when overexpressed in cells (Chan *et al*, 2000; Yang *et al*, 2000; Volchkov *et al*, 2001). In this respect, it is important to note that the highly pathogenic Zaire EBOV differs in the amino-acid sequence at the shedding site from other subtypes, including the apathogenic Reston EBOV. Whether these sequence variations are reflected by differences in shedding efficiency should be investigated in future studies using recombinant Ebola viruses (Volchkov *et al*, 2001).

Detection of truncated GP_2 in the blood of infected animals proves that GP shedding occurs not only in cell culture but also in *in vivo* infection. Comparison of the relative amounts of $GP_{2\Delta}$ and VP40 in cell culture medium and in sera suggests that the shedding rate in animals is dramatically higher than in Vero cells. There is increasing evidence for immunosuppression in lethal EBOV infection, which in part is explained by infection of monocytes and macrophages, the primary targets of the virus (Ryabchikova *et al*, 1996; Hensley *et al*, 2002). However, the disease is also characterized by an inability of the immune system to recognize virus-infected cells. Electron microscopical data obtained with EBOV-infected animals indicated that there was almost no immune attack on infected and virus-producing cells. In spite of extensive necrosis and massive virus reproduction, tissues showed no inflammatory reactions. $GP_{1,2\Delta}$ released from infected cells very likely contributes to this immune suppression by absorbing antibodies that otherwise interact with virus or virus-infected cells. This is indicated by our observations that $GP_{1,2\Delta}$ is shed in infected guinea pigs and that it is recognized by the human monoclonal antibody KZ52. This antibody binds to GP on virions and on the surface of infected cells, neutralizes EBOV in cell culture, and protects guinea pigs from lethal EBOV infection (Parren *et al*, 2002). However, the protection of guinea pigs required a high dose of KZ52 antibody administered close to the time of virus challenge. This could, again, be explained by a decoy function of shed GP blocking the virus-neutralizing activity of KZ52. For the same reason, attempts to protect monkeys by passive transfer of antibodies may have failed (Jahrling *et al*, 1996). It appears, however, that the decoy problem no longer exists in the presence of high antibody titers and a strong T-cell response against GP as is the case after protective immunization of monkeys with a vaccine based on replication-defective adenovirus (Sullivan *et al*, 2003).

We have previously reported that soluble GP_1 devoid of GP_2 is secreted from HeLa cells, presumably resulting from the release of the disulfide bond linking both subunits (Volchkov *et al*, 1998a). However, since soluble GP_1 has neither been detected in cell culture fluid from several other cell lines nor in infected animals, it is unlikely to play a major biological role. Similarly, it is questionable if the secreted glycoprotein sGP, which has also been speculated to act as a decoy (Sanchez *et al*, 1996; Ito *et al*, 2001), is a suitable candidate for this function, since despite sharing most of its amino-acid sequence with the envelope glycoprotein it significantly differs in tertiary and quaternary structures (Volchkova *et al*, 1998; Sanchez *et al*, 1998). Furthermore, the glycoprotein of Marburg virus, another member of the *Filoviridae* family causing a similar disease, is also shed from infected cells (VE Volchkov, unpublished results), whereas sGP is not expressed in this case due to a different *GP* gene organization. This also underlines the role of GP shedding as an important factor in pathogenesis.

In conclusion, we show that the ectodomain of EBOV GP is released in soluble form from the cell surface following proteolytic cleavage with involvement of ADAMs and particularly TACE. To our knowledge, this is the first description of the shedding mechanism of a viral membrane glycoprotein. It is likely that other viruses shed their surface glycoproteins in a similar manner with the same enzyme involvement. Our observations that a significant amount of shed GP is present in the blood of infected animals and that $GP_{1,2\Delta}$ can effectively block neutralizing antibodies provide evidence for a novel viral escape mechanism from the host's immune response. It is feasible to postulate that shed GP has other functions in addition to acting as a decoy. Shed GP may well interact with several types of cells involved in Ebola pathogenicity, and this is an area for further investigations.

Materials and methods

Viruses and cell cultures

The Mayinga strain of EBOV, subtype Zaire (provided by CDC, Atlanta) and EBOV adapted to guinea pigs were propagated in Vero E6 cells. The vaccinia virus strain WR and recombinant vaccinia viruses vTF7-3 expressing T7 RNA polymerase (provided by B Moss, NIH, Bethesda) and vSCGP8 expressing EBOV GP (Volchkov *et al*, 1995) were propagated in CV-1 cells. RK-13, CV-1, HeLa, 293, and Vero cells were cultured at conditions recommended by ATCC. EC-2 cells, $TACE^{\Delta Zn/\Delta Zn}$-deficient mouse fibroblasts (provided by RA Black, Amgen), were maintained in Dulbecco's modified Eagle's medium and Ham's F-12 medium supplemented with 10% FCS.

Pulse-chase labeling and immunoprecipitation

Cells (1×10^6) were infected with recombinant vaccinia viruses expressing EBOV GP at a multiplicity of infection (moi) of 10 PFU/cell for 1 h at 37°C or transfected with recombinant plasmids (3 μg, 10 μl lipofectin). Cells were washed 6–10 h post infection (p.i.) or 18–36 h post transfection (p.t.), starved in methionine–cysteine-free medium, and labeled with 100 μCi/ml [^{35}S]cysteine (Amersham). After a 30 min pulse, cells were chased for different time intervals. Supernatants were collected and cells lysed in Co-IP buffer (1% NP-40, 0.4% deoxycholate (DOC), 5 mM EDTA, 100 mM NaCl, 20 mM Tris–HCl, pH 7.6, 25 mM iodacetamide, 1 mM PMSF). Nuclei and insoluble debris were removed by centrifugation at 14 000 rpm and 4°C. Immunoprecipitation of proteins was performed using either horse anti-EBOV immunoglobulins (Igs) and protein A–sepharose conjugated with rabbit anti-horse Igs or human EBOV-neutralizing antibody KZ52 (Volchkov *et al*, 1998a). Samples were subjected to SDS–PAGE, the gels dried, autoradiographed, and analyzed on a Bas 2000 Bio-Imager (RayTest).

Oligomerization analysis

Vero E6 cells were infected with EBOV at an moi of 10^{-2} PFU/cell, and culture medium was collected 5 days p.i. Medium was clarified by low-speed centrifugation and virus was pelleted through a 20% sucrose cushion by ultracentrifugation (Beckman SW28 rotor, 25 000 rpm, 1 h, 4°C). Pelleted virus and supernatant were solubilized with 1% NP-40 and 0.4% DOC and subjected to ultracentrifugation (Beckman SW41 rotor, 270 000 g, 19 h, 10°C)

through a linear 5–25% (w/w) sucrose gradient prepared with Co-IP buffer. Fractions were collected from the bottom to the top, proteins separated by SDS–PAGE and analyzed by Western blot using rabbit ant-GP$_2$ Igs (1:2000) and horseradish peroxidase (HRP)-conjugated goat anti-rabbit antibody (1:30 000). Detection was performed with enhanced chemoluminescence (ECL) technique (Perbio Science) following the manufacturer's instructions.

Surface biotinylation

RK-13 cells were infected with vSCGP8 at an moi of 10 PFU/cell. At 10 h p.i., cells were washed with PBS and incubated twice for 20 min with 2 mg Sulfo-NHS-Biotin (Calbiochem) in PBS at 4°C. Unbound biotin was blocked with 100 mM glycine. To monitor the release of surface proteins into medium, cells were incubated at 37°C and culture medium and cells were collected at different time intervals. Biotin-labeled proteins from supernatants obtained after ultracentrifugation (25 000 rpm, 1 h, 4°C) of medium and cells lysed in CO-IP buffer were immunoprecipitated with anti-EBOV Igs. Samples were analyzed by Western blot using streptavidin-coupled HRP and the ECL technique.

Site-directed mutagenesis and construction of recombinant vaccinia viruses

Single or multiple amino-acid exchanges and deletions in GP encoded by pSC-mGP8 or pGEM-mGP8 were introduced by site-directed mutagenesis (Stratagene). The construction of recombinant vaccinia viruses expressing EBOV GP mutants was performed as described elsewhere (Volchkov *et al*, 1995).

Shedding inhibition assay

For shedding inhibition studies, cells infected with vSCGP8 were pulse-chase labeled and incubated for 8 h either with or without protease inhibitors. Culture medium and cells were subjected to immunoprecipitation analysis. Inhibitors used were as follows: TIMP-1, TIMP-2, BB2516, GM6001, MMP-3 inhibitor II, MMP-8 inhibitor I and MMP-2 inhibitor (Calbiochem), TIMP-3 and TIMP-4 (Chemicon International), α-antichymotrypsin, captopril, EDTA, EGTA, 1,10-phenanthroline and phosphoramidon (Sigma), TAPI-I (Peptides International), and CGS 27023 (kindly provided by H Eckhardt, Novartis Pharmaceuticals).

Antisense oligonucleotide treatment

Antisense oligonucleotides (ASOs) were synthesized by Sigma and designed to hybridize to human *TACE* mRNA. The ASOs contained five 2′-*O*-methyl modifications on the 5′- and 3′-ends and were uniformly modified with phosphorothioate linkages. Sequences used were as follows: ASO2—TCAGCATTTCGACGTTACTG; ASO4—CCCTAGTCAGTGCTGTTAT; ASO5—CCTACTGTACAGGGCTTTCC; ASO2M—TCAGCTTCTCAACATTACTG; ASO4M—CCCTAGTGATTTCAGTTATC (mismatch residues are underlined). 293 cells were infected with vSCGP8 at an moi of 10 PFU/cell and subsequently transfected with ASOs at a final concentration of 10 μM using lipofectin (Gibco). At 7 h p.t., cells were labeled and chased for 8 h. Labeled proteins from cells and culture medium were subjected to immunoprecipitation analysis.

Purification of soluble GP and cleavage site determination

Vero E6 cells were infected with EBOV at an moi of 10^{-2} PFU/cell. Culture medium was subjected to ultracentrifugation (Beckman

SW28 rotor, 25 000 rpm, 1 h, 4°C) 5 days p.i. Supernatants were collected and incubated with anti-GP$_2$ antibodies crosslinked with protein A–sepharose overnight at 4°C. For chromatography, columns were filled with sepharose beads, and washed with 10 column volumes of 10 mM Tris–HCl buffer (pH 7.5). GP was eluted in 2 ml fractions with 100 mM Na-citrate buffer (pH 3.0), and fractions were analyzed by Western blot using anti-GP$_2$ antibody. Fractions containing GP were combined and incubated at 4°C with wheat germ lectin agarose (Pharmacia). The agarose was washed with 50 mM Tris–HCl buffer (pH 8.0) containing 10 mM *N*-acetyl-glucosamine, and GP was eluted in 2 ml fractions with 50 mM Tris–HCl buffer (pH 8.0) containing 200 mM *N*-acetyl-glucosamine and analyzed with the SilverQuest™ Staining Kit (Invitrogen). For matrix-associated laser desorption ionization time-of-flight mass spectrometry (MALDI-TOF MS), purified GP was concentrated (centriplus-50, Millipore), deglycosylated with 15 000 U PNGase F (Biolabs), and treated with 10 mM DTT (1 h, 50°C) and then with 50 mM iodoacetamide (30 min, 25°C). Samples were further concentrated (centricon-10, Millipore) and combined with a saturated sinapin acid solution (1:1 ratio) containing 0.1% trifluoroacetic acid and 67% acetonitrile for co-crystallization. MALDI-TOF MS was carried out with the Voyager-DE RP Biosystem.

Neutralization inhibition assay

Two-fold serial dilutions of EBOV stock (3.5×10^4 PFU/ml) were prepared on DMEM. Virus dilutions were preincubated with human EBOV-neutralizing antibody KZ52 at a final concentration of 0.6 μg/ml, or with purified shed GP at different concentrations, or with a mixture of KZ52 and shed GP for 1 h at room temperature. Vero E6 cells were then inoculated with 100 μl of each mixture. Cells infected with different EBOV dilutions were used as controls. Cells were treated with 4% paraformaldehyde 30 h p.i., permeabilized with 0.1% Triton X-100, and incubated with mouse monoclonal anti-NP antibody (1:300) and then with peroxidase-conjugated sheep-anti-mouse antibody (1:1000). Infectious units (single blue cells or groups of stained cells) were visualized after incubation with TrueBlue™ peroxidase substrate (KPL) and counted per well.

Supplementary data

Supplementary data are available at *The EMBO Journal* Online.

References

Althoff K, Müllberg J, Aasland D, Voltz N, Kallen KJ, Grötzinger J, Rose-Hohn S (2001) Recognition sequences and structural elements contribute to shedding susceptibility of membrane proteins. *Biochem J* **353:** 663–672

Althoff K, Reddy P, Voltz N, Rose-John S, Müllberg J (2000) Shedding of interleukin 6 receptor and tumor necrosis factor alpha: contribution of the stalk sequence to the cleavage pattern of transmembrane proteins. *Eur J Biochem* **267:** 2624–2631

Alvarez CP, Lasals F, Carrillo J, Muñiz O, Corbí AL, Delgado R (2002) C-type lectins DC-SIGN and L-SIGN mediate cellular entry by Ebola virus in *cis* and in *trans*. *J Virol* **76:** 6841–6844

Bavari S, Bosio CM, Wiegand E, Ruthel G, Will AB, Geisbert TW, Hevey M, Schmaljohn C, Schmlajohn A, Aman MJ (2002) Lipid

rafts microdomains: a gateway for compartmentalized trafficking of Ebola and Marburg viruses. *J Exp Med* **195:** 593–602

Black RA, Rauch CT, Kozlosky CJ, Peschon JJ, Slack JL, Wolfson MF, Castner BJ, Stocking KL, Reddy P, Srinivasan S, Nelson N, Boiani N, Schooley KA, Gerhart M, Davis R, Fitzner JN, Johnson RS, Paxton RJ, March CJ, Cerretti DP (1997) A metalloproteinase desintegrin that releases tumor-necrosis factor-alpha from cells. *Nature* **385:** 729–733

Blobel CP (2000) Remarkable roles of proteolysis on and beyond the cell surface. *Curr Opin Cell Biol* **12:** 606–612

Blobel CP (2002) Functional and biochemical characterization of ADAMs and their predicted role in protein ectodomain shedding. *Inflamm Res* **51:** 83–84

Brou C, Logeat F, Gupta N, Bessia C, LeBail O, Doedens JR, Cumano A, Roux P, Black RA, Israel A (2000) A novel proteolytic cleavage involvement in Notch signaling: the role of the disintegrin-metalloprotease TACE. *Mol Cell* **5:** 207–216

Buxbaum JD, Liu KN, Lou Y, Slack JL, Stocking KL, Peschon JJ, Johnson RS, Caster BJ, Cerretti DP, Black RA (1998) Evidence that tumor necrosis factor alpha converting enzyme is involved in regulated α-secretase cleavage of the Alzheimer amyloid protein precursor. *J Biol Chem* **273:** 27765–27767

Chan SY, Empig CJ, Welte FJ, Speck RF, Schmaljohn A, Kreisberg JF, Goldsmith MA (2001) Folate receptor-α is a cofactor for cellular entry by Marburg and Ebola viruses. *Cell* **106:** 117–126

Chan SY, Ma MC, Goldsmith MA (2000) Differential induction of cellular detachment by envelope glycoproteins of Marburg and Ebola (Zaire) viruses. *J Gen Virol* **81:** 2155–2159

Ehlers MRW, Schwager SLU, Scholle RR, Manji GA, Brandt WF, Riordan JF (1996) Proteolytic release of membrane-bound angiotensin-converting enzyme: role of the juxtamembrane stalk sequence. *Biochemistry* **35:** 9549–9559

Elliott MJ, Naini RN, Feldmann M, Kalden JR, Antoni C, Smolen JS, Leeb B, Breedveld FC, Macfarlane JD, Bijl H (1994) Randomized double-blind comparison of chimeric monoclonal antibody to tumor necrosis factor alpha (cA2) versus placebo in rheumatoid arthritis. *Lancet* **344:** 1105–1110

Grünberg J, Kruppa A, Paschen P, Kruppa J (1991) Intracellular formation of two soluble glycoproteins in BHK cells infected with Vesicular Stomatitis Virus serotype New Jersey. *Virology* **180:** 678–686

Hensley LE, Young HA, Jahrling PB, Geisbert TW (2002) Proinflammatory response during Ebola virus infection of primate models: possible involvement of the tumor necrosis factor receptor superfamily. *Immunol Lett* **80:** 169–179

Hooper NM, Karran EH, Turner AJ (1997) Membrane protein secretases. *Biochem J* **321:** 265–279

Ito H, Watanabe S, Sanchez A, Whitt MA, Kawaoka Y (1999) Mutational analysis of the putative fusion domain of Ebola virus glycoprotein. *J Virol* **7:** 8907–8912

Ito H, Watanabe S, Takada A, Kawaoka Y (2001) Ebola virus glycoprotein: proteolytic processing, acylation, cell tropism, and detection of neutralizing antibodies. *J Virol* **75:** 1576–1580

Jahrling PB, Geisbert J, Swearengen JR, Jaax GP, Lewis T, Huggins JW, Schmidt JJ, LeDuc JW, Peters CJ (1996) Passive immunization of Ebola virus-infected cynomolgus monkeys with immunoglobulin from hyperimmune horses. *Arch Virol* **11** (Suppl)**:** 135–140

Jeffers SA, Sanders DA, Sanchez A (2002) Covalent modifications of the Ebola virus glycoprotein. *J Virol* **76:** 12463–12472

Malvoisin E, Wild F (1994) Characterization of a secreted form of measles virus haemagglutinin expressed from a vaccinia virus recombinant. *J Gen Virol* **75:** 3606–3609

Maruyama T, Rodriguez LL, Jahrling PB, Sanchez A, Khan AS, Nichol ST, Petres CJ, Parren PW, Burto DR (1999) Ebola virus can be effectively neutralized by antibody produced in natural human infection. *J Virol* **73:** 6024–6030

Morimoto K, Iwatani Y, Kawai A (1993) Shedding of G_s protein (a soluble form of the viral glycoprotein) by the rabies virus-infected BHK-21 cells. *Virology* **195:** 541–549

Müllberg J, Althoff K, Jostock T, Rose-John S (2000) The importance of shedding of membrane proteins for cytokine biology. *Eur Cytokine Netw* **11:** 27–37

Parren PW, Geisbert TW, Maruyama T, Jahrling PB, Burton DR (2002) Pre- and postexposure prophylaxis of Ebola virus infection in an animal model by passive transfer of a neutralizing human antibody. *J Virol* **76:** 6408–6412

Peschon JJ, Slack JL, Reddy P, Stocking KL, Sunnarborg SW, Lee DC, Russell WE, Castner BJ, Johnson RS, Fitzner JN, Boyce RW, Nelson N, Kozlosky CJ, Wolfson MF, Rauch CT, Cerretti DP, Paxton RJ, March CJ, Black RA (1998) An essential role for ectodomain shedding in mammalian development. *Science* **282:** 1281–1284

Peters CJ (1996) Emerging infections—Ebola and other filoviruses. *West J Med* **164:** 36–38

Reddy P, Slack JL, Davis R, Cerretti DP, Kozlosky CJ, Blanton RA, Shows D, Peschon JJ, Black RA (2000) Functional analysis of the domain structure of tumor necrosis factor-α converting enzyme. *J Biol Chem* **275:** 14608–14614

Roberts SR, Lichtenstein D, Ball LA, Wertz GW (1994) The membrane-associated and non-associated forms of the respiratory syncytial virus attachment glycoprotein G are synthesized from alternative initiation codons. *J Virol* **68:** 4538–4546

Rose-John S, Heinrich PC (1994) Soluble receptors for cytokines and growth factors: generation and biological function. *Biochem J* **300:** 281–290

Ryabchikova EI, Kolesnikova L, Smolina M, Tkachev V, Pereboeva L, Baranova S, Grazhdantseva A, Rassadkin Y (1996) Ebola virus infection in guinea pigs: presumable role of granulomatous inflammation in pathogenesis. *Arch Virol* **141:** 909–921

Sanchez A, Trappier SG, Mahy BW, Peters CJ, Nichol ST (1996) The virion glycoproteins of Ebola viruses are encoded in two reading frames and are expressed through transcriptional editing. *Proc Natl Acad Sci USA* **93:** 3602–3607

Sanchez A, Yang ZY, Xu L, Nabel GJ, Crews T, Peters CJ (1998) Biochemical analysis of the secreted and virion glycoproteins of Ebola virus. *J Virol* **72:** 6442–6447

Schlondorf J, Blobel C (1999) Metalloprotease-disintegrins: modular proteins capable of promoting cell–cell interactions and triggering signals by protein ectodomain shedding. *J Cell Sci* **112:** 3603–3617

Sullivan NJ, Geisbert TW, Geisbert JB, Xu L, Yang ZY, Roederer M, Koup RA, Jahrling PB, Nabel GJ (2003) Accelerated vaccination for Ebola virus haemorrhagic fever in non-human primates. *Nature* **424:** 681–684

Van Dullemen HM, van Deventer SJ, Hommes DW, Bijl HA, Jansen J, Tytgat GN, Woody J (1995) Treatment of Crohn's disease with anti-tumor necrosis factor chimeric monoclonal antibody (cA2). *Gastroenterology* **109:** 129–135

Volchkov VE, Becker S, Volchkova VA, Ternovoj VA, Kotov AN, Netesov SV, Klenk HD (1995) GP mRNA of Ebola virus is edited by the Ebola virus polymerase and by T7 and vaccinia virus polymerase. *Virology* **214:** 421–430

Volchkov VE, Chepurnov AA, Volchkova VA, Ternovoj VA, Klenk HD (2000) Molecular characterization of guinea pig-adapted variants of Ebola virus. *Virology* **277:** 147–155

Volchkova VA, Feldmann H, Klenk HD, Volchkov VE (1998) The nonstructural small glycoprotein sGP of Ebola virus is secreted as an anti-parallel orientated homodimer. *Virology* **250:** 408–414

Volchkov VE, Feldmann H, Volchkova VA, Klenk HD (1998b) Processing of the Ebola virus glycoprotein by the proprotein convertase furin. *Proc Natl Acad Sci USA* **95:** 5762–5767

Volchkov VE, Volchkova VA, Mühlberger E, Kolesnikova LV, Weik M, Dolnik O, Klenk HD (2001) Recovery of infectious Ebola virus from complementary DNA: RNA editing of the GP gene and viral cytotoxicity. *Science* **291:** 1965–1969

Volchkov VE, Volchkova VA, Slenczka W, Klenk HD, Feldmann H (1998a) Release of viral glycoprotein during Ebola virus infection. *Virology* **245:** 110–119

Yang Z, Delgado R, Xu L, Todd RF, Nabek EG, Sanchez A, Nabel GJ (1998) Distinct cellular interactions of secreted and transmembrane Ebola virus glycoproteins. *Science* **279:** 1034–1036

Yang ZY, Duckers HJ, Sullivan NJ, Sanchez A, Nabel EG, Nabel GJ (2000) Identification of the Ebola virus glycoprotein as the main viral determinant of vascular cell cytotoxicity and injury. *Nat Med* **8:** 886–889